Influence of the salt concentration on the damage potential of mirabilite and thenardite

A. Stahlbuhk*, J. Nissen, K. Linnow and M. Steiger
Department of Chemistry, University of Hamburg,
Inorganic and Applied Chemistry, Hamburg Germany
* Amelie.stahlbuhk@studium.uni-hamburg.de

Abstract

The present study reports on the damage potential of the crystallization of either thenardite or mirabilite in porous sandstone. Specimens of Sand sandstone with different loads of sodium sulfate were exposed to wetting-drying cycles at different conditions to rank the damage potential of different crystallization pathways and to investigate the influence of the salt concentration on the damage process. The damage intensity was assessed by visual inspection and mass loss curves. In general, the well-known extreme damage potential of thenardite dissolution and subsequent mirabilite crystallization is confirmed. Under such conditions, the damage potential increases with increasing salt load which is confirmed by the calculation of the effective stresses and comparison with the tensile strength of Sand sandstone. Considering the pore filling ratio with respect to the crystallizing phase, it turns out that thenardite crystallization during evaporation can cause as much damage as the crystallization of mirabilite during wetting of thenardite. Finally, it is demonstrated that wetting by slow deliquescence of thenardite can also be very destructive, though it is yet unclear which phases actually crystallize out under such conditions.

Keywords: damage potential, thenardite, mirabilite, salt concentration, pore filling ratio

1 Introduction

Precipitation of salts in contact with their supersaturated solution is the key mechanism for damage to porous materials. Sodium sulfate has been repeatedly reported as one of the most aggressive salts. Although sodium sulfate is commonly used in laboratory weathering tests, little is known about the influence of different crystallization pathways and the influence of the salt concentration on the damage potential. In general the interaction between a salt, the material and the climatic conditions related to the manifestation of damage is complicated. The interactions of the different influences are given schematically in Figure 1. The damage is influenced by the crystallization pressure and the mechanical properties of the stone, i.e. the tensile strength. The theoretical crystallization pressure can be calculated if the supersaturation of the crystallizing phase is known [1]. To relate the crystallization pressure to the macroscopic stress, the pore filling ratio must be taken into account because the theoretical pressure is not effectively transmitted through a porous material when the pores are not sufficiently filled with crystals [2,3]. The supersaturation during growth depends on the crystallization pathway and might change according to the climatic conditions, e.g. evaporation or cooling rates, and the presence of nucleation sites within the material.

Typically, in laboratory tests a porous material is repeatedly impregnated with a sodium sulfate solution at room temperature (r.t.) and dried at a higher temperature. For a long time damage was attributed to the volume increase associated with the hydration reaction. Today, it is well known that the damage is due to the growth of mirabilite ($Na_2SO_4 \cdot 10H_2O$) crystals from the supersaturated solution formed by the dissolution of thenardite (Na_2SO_4). Such a dissolution-crystallization mechanism not only occurs during wetting by impregnation but also during wetting at relative humidities above the deliquescence humidity of thenardite. Direct hydration without formation of a solution is also possible [4]. However, up to now the damage potential of this reaction is not well investigated,

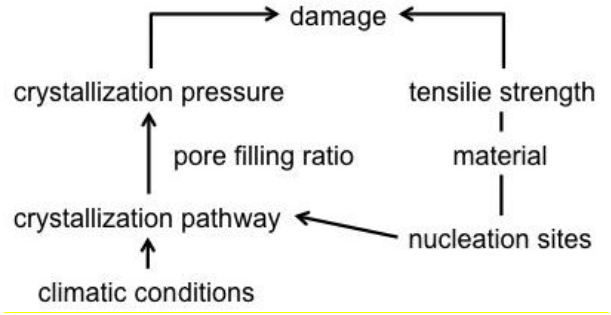

Figure 1: Overview of the aspects influencing the magnitude of damage.

whereas several investigations showed that dissolution of thenardite and recrystallization of mirabilite is extremely destructive [e.g. 5,6].

In a recent study [7] it was shown that the crystallization of sodium sulfate phases from a saturated solution can in fact lead to severe degradation patterns, even in the absence of temperature or wet/dry cycles. In contrast, another study shows that thenardite crystallization during evaporation produces less damage than the thenardite dissolution - mirabilite crystallization mechanism occurring during wetting [8]. However, comparing the two salts it is often ignored that, for a given sodium sulfate content in a porous material, the pore filling ratio of thenardite is much lower than that of mirabilite. For example, repeated impregnations with a solution saturated with respect to mirabilite at room temperature are often used to enhance the damage. The pore filling ratio increases with the cycle number. Assuming complete saturation of the pore space, repeated impregnations at 20 °C with a saturated solution (1.35 $mol \cdot kg^{-1}$) lead to pore filling ratios of 29 %, 49 %, 64 %, 74 % and 82 % with respect to mirabilite in the first, second, third, fourth and fifth cycle, respectively.

The same concentration is often used to investigate the damage potential of thenardite alone. In the first cycle the pore filling ratio of 29 % is then reduced to 7 %, i.e. by a factor of 4.1, with respect to thenardite. In the following cycles during the impregnation above 32.4 °C thenardite dissolves in the brine due to the undersaturation with respect to thenardite (saturation concentration of 3.51 $mol \cdot kg^{-1}$ at 32.4 °C) of the used brine. It follows that the increase of the pore filling ratio is less steep than for mirabilite at 20 °C. Therefore the damage produced by mirabilite crystallization has to be more pronounced in these investigations simply because there is a much higher pore filling.

For this reason, the present study has two objectives, a ranking of different crystallization pathways involving both thenardite and mirabilite, and, the investigation of the influence of the salt concentration on the damage potential. For this purpose, Sand sandstone samples with different sodium sulfate concentrations were exposed to four different wetting-drying cycles. The first set of samples was both wetted with liquid water and dried at 40 °C to avoid the formation of mirabilite during wetting as well as during drying. The second set of samples was wetted with liquid water at temperature of the lab (22–26 °C) to induce the crystallization of mirabilite during wetting. The third set was exposed at 90 % RH at temperature of the lab, above the deliquescence humidity of thenardite to induce mirabilite crystallization from its supersaturated solution. Finally, the fourth set was exposed at 84 % RH at temperature of the lab below the deliquescence humidity of thenardite but above the equilibrium humidity of the thenardite-mirabilite transition. In this case, the hydration should occur as a true solid state reaction without dissolution.

2 Materials and methods

2.1 Sample preparation

Sand sandstone (Middle Keuper) was cut into blocks with the dimension of 30 x 30 x 15 mm^3. The major constituents of this sandstone are quartz, rock fragments, plagioclase and alkali feldspars. The porosity is 20 %v/v and the bulk density is 2.13 $g \cdot cm^{-3}$ [9]. Exchangeable cations in Sand sandstone [10] were replaced with sodium immersing the specimens in a sodium sulfate solution (1.35 $mol \cdot kg^{-1}$). This solution was replaced three times. To remove excess sodium sulfate, the samples were subsequently washed three times by immersion in doubly distilled water. Different salt loads were achieved by impregnation with salt solutions of different concentrations. For low salt content, solutions of 0.32, 0.68 and 1.35 $mol \cdot kg^{-1}$ were used, whilst higher loads were obtained by one or up to three impregnations with a 3.2 $mol \cdot kg^{-1}$ solution. These impregnations were carried out at 40 °C to avoid the formation of mirabilite during the impregnation. All specimens were dried at 130 °C after each impregnation.

2.2 Climatic conditions of the cycling

The cycles were carried out at four different conditions. Each cycle started with the wetting of the specimen and ended with complete drying. Depending on the temperature and the method used for wetting, different mechanisms of damage should affect the stones. Regarding the thermodynamic stabilities in the Na_2SO_4—H_2O system, mirabilite cannot be formed above 32.4 °C. Thus, in order to study the influence of thenardite crystallization, repeated cycles of wetting and drying, both at 40 °C, were carried out (A_{then}). At room temperature, thenardite forms a saturated solution and subsequently mirabilite precipitates from its supersaturated solution (method B_{mir}). Wetting with water vapor may induce two different hydration mechanisms [4]. Above the deliquescence humidity of thenardite a dissolution re-crystallization mechanism takes place in addition to the solid gas reaction (method C_{mir}), where the specimens were stored during the wetting process in a desiccator above a saturated $MgSO_4$ solution (90% RH). Below the deliquescence humidity of thenardite (86–87 % RH at 20–25 °C) the hydration takes place as a true solid state reaction, which was found to be incomplete for the pure salt [4]. In order to study this process the specimens were stored in a desiccator above a saturated KCl solution at about 84% RH (method D_{mir}). The reaction equations of the different methods are summarized in Figure 2.

The amount of liquid water for the wetting in methods A_{then} and B_{mir} was adapted to the salt load of each specimen to allow the full hydration of thenardite to mirabilite. The calculated volume varies from 10 µL to 589 µL. It turns out that the penetration of the pipetted water takes some time during which evaporation takes place. To compensate for this evaporative loss, an additional 100 µL was added to the samples.

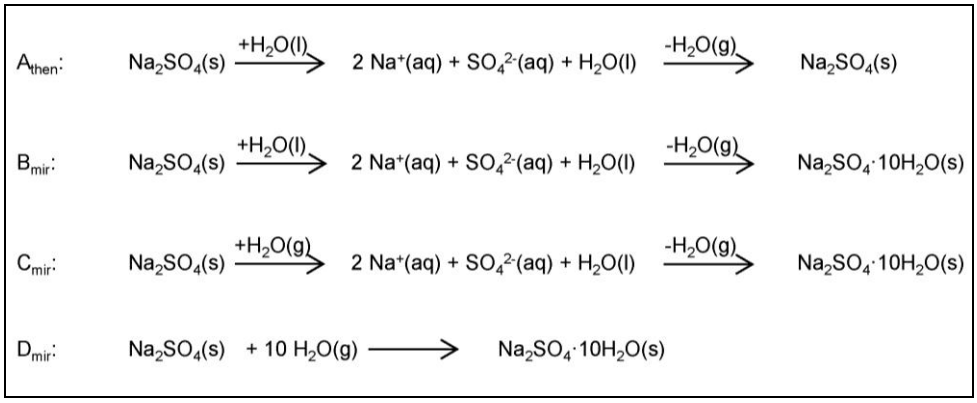

Figure 2: Overview of the cycling methods and the relevant reaction mechanism.

After wetting, samples of method A_{then} were dried in a desiccator above silica at 40 °C till constant weight, while those of methods B_{mir}, C_{mir} and D_{mir} in a desiccator above silica at temperature of the lab. In addition a flow of dry air was used to reduce the drying times (methods B_{mir}, C_{mir}, and D_{mir}).The mass of the dried specimens was measured after each cycle. The damage in the specimens having different salt loads is assessed by the mass decrease with ongoing cycling and visual observations. One sample was tested for each method and salt load. The total cycle number is up to 17.

3 Results and discussion

3.1 Load and visual appearance after impregnation

Obvious damage of the specimens and efflorescences were not visible after the initial impregnation and drying procedure. The average salt loads of equally impregnated stones and the pore filling of each individual specimen are given in Table 1. These pore fillings are only average values that do not reflect the fact that gradients of salt concentration, hence, the pore filling evolve during drying.

3.2 Damage

Visual rating (Table 2)

In general the damage appeared in different forms, which can be described as sanding, crumbling, formation of big cracks and total breakdown of the specimens. The localization of salt deposit played a major role on the visible damage. Specimens of method A_{then} did not show

any efflorescences (see for example Figure 3a) and mostly do not show visually detectable damage such as rounding of the corners and edges by sanding, or crumbling. Damage was only observed for the specimen A8, where a big crack was observed after cycle 4. With ongoing cycling the crack enlarged accompanied by sanding and ended in the total breakdown of the sample after cycle 6, obviously caused by subflorescences.

Table 1: Average salt load of the specimens, given in mg Na_2SO_4 per g stone, with the standard deviation of the mean value, and average pore filling ratio Φ with respect to the crystal volume of the damaging phase.

Specimen	salt load ($mg \cdot g^{-1}$)	A_{then} Φ_{then} (%)	B_{mir} Φ_{mir} (%)	C_{mir} Φ_{mir} (%)	D_{mir} Φ_{mir} (%)
1	0.55 ± 0.05	0.20	1.00	–(1)	–(1)
2	2.2 ± 0.2	0.86	4.03	3.47	3.62
3	4.3 ± 0.8	1.74	7.25	8.50	6.04
4	10.5 ± 1.3	4.10	16.9	19.6	16.01
5	13.9 ± 0.5	5.65	22.6	23.7	22.23
6	24.5 ± 2.5	9.24	39.3	–(1)	–(1)
7	31.1 ± 1.8	12.2	54.8	50.4	50.9
8	44.8	17.8	–(1)	–(1)	–(1)

(1): not tested

Table 2: Cycle number at which visible damage is observed.

Specimen	A_{then}	B_{mir}	C_{mir}	D_{mir}
1	> 6(1)	> 6(1)	–(2)	–(2)
2	> 5(1)	> 5(1)	> 5(1)	> 5(1)
3	> 17(1)	> 7(1)	> 9(1)	> 9(1)
4	> 17(1)	9 (sanding)	> 9(1)	> 9(1)
5	> 17(1)	4 (sanding)	> 9(1)	> 9(1)
6	> 6(1)	3 (small cracks)	–(2)	–(2)
7	> 3(1)	1 (small cracks) 3 (breakdown)	> 5(1)	2 (big crack) 4 (breakdown)
8	4 (big crack) 6 (breakdown)	–(2)	–(2)	–(2)

(1): > n: no damage observed after n cycles
(2): not tested

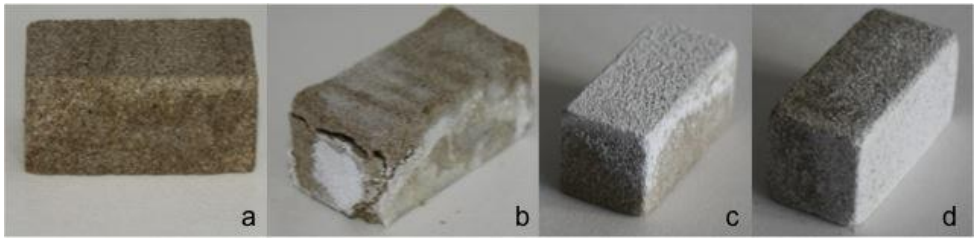

Figure 3: Damage of different specimens; a) A6 after the fourth cycle, b) B6 after the fourth cycle, c) C5 after the eighth cycle and d) D4 after the eighth cycle.

All specimens of method B_{mir} showed some efflorescences and damage in the form of sanding and loss of debris. Rounded edges and corners and loss of small particles were clearly visible on specimens B4–B7, whilst B1–B3 showed no damage. In addition, small cracks formed in samples B6 and B7 after the third and the first cycle, respectively. With ongoing cycling the cracks enlarged. As an example, specimen B6 is shown in Figure 3b after the fourth cycle, illustrating the enhanced cracks. The total breakdown of B7 occurred in the third cycle during wetting. A huge amount of sodium sulfate was present as efflorescences on the specimens subjected to conditions of method C_{mir} (see example in Figure 3c) and those with a high salt load are nearly fully covered by fine salt grains. As no efflorescence was noticed after impregnation, its appearance evidenced the formation and transport of a salt solution as expected in a deliquescence-recrystallization mechanism. However, no damage was observed on the specimens subjected to conditions of method C_{mir}.

Surprisingly, the specimens of method D_{mir} also showed efflorescences after some cycles (see Figure 3d as an example), despite an expected solid state hydration mechanism as the RH is below the deliquescence humidity of thenardite. As mentioned before the formation of efflorescences gives evidence of the presence of a solution which may be formed due to the water vapor sorption behavior of the stone itself, the secondary porosity of the thenardite grains or the presence of Na_2SO_4(III) (phase III) which deliquesces at about 83 % RH (20–25 °C). Damage was only observed in the specimen with the highest salt load (D7). The formation of a big crack after cycle 2 ended in the total breakdown of the sample after cycle 4.

Mass loss

The specimens were dried until constant weight at the end of each cycle. The normalized weight w_n was calculated by Equation (1):

$$w_n = \frac{m_i}{m_0} \quad (1)$$

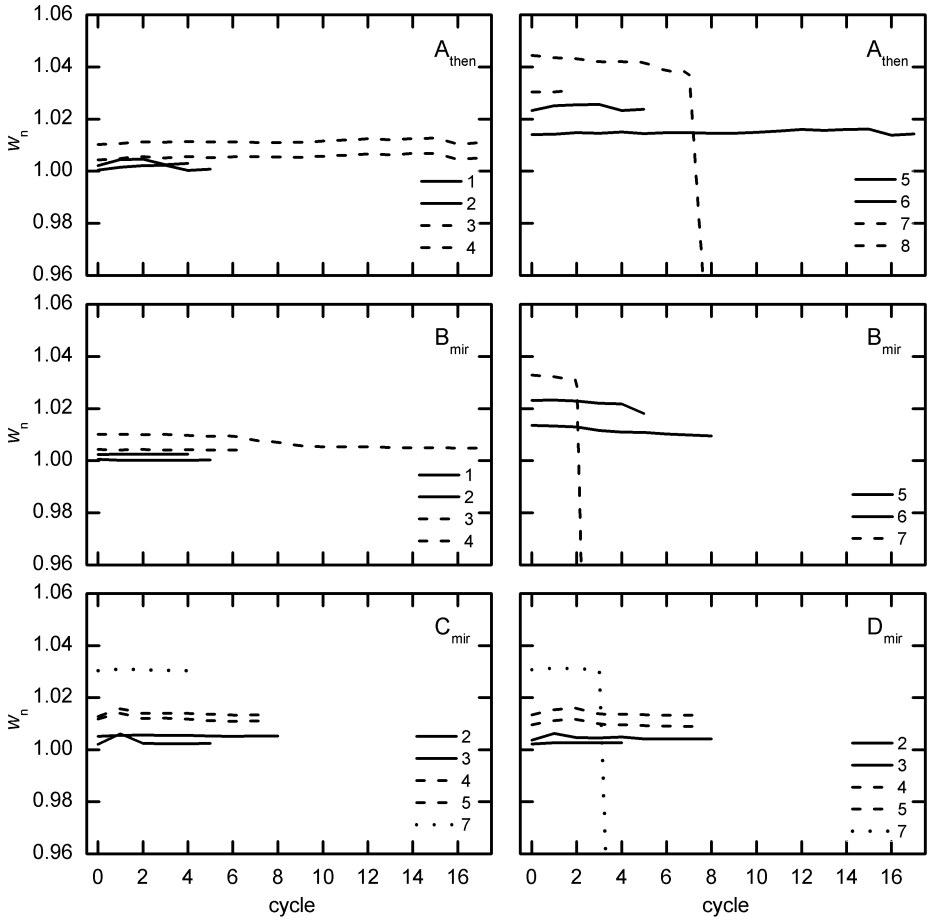

Figure 4: Normalized weight w_n with ongoing cycling.

where m_i is the dry weight after each cycle and m_0 the dry mass of the untreated sample. The evolution of the normalized weight is depicted in Figure 4. The number of cycles is not the same for all methods as some experiments were started later (A1,2,6,7; B1–3,5,6; C2,7; D2,7).

Moreover, the water uptake of the specimens subjected to conditions of methods C_{mir} and D_{mir} was very slow, thus, substantially increasing the total time required for a complete cycle. Figure 5 depicts the time consuming water sorption of sample D7 that finally lasted 20 days.

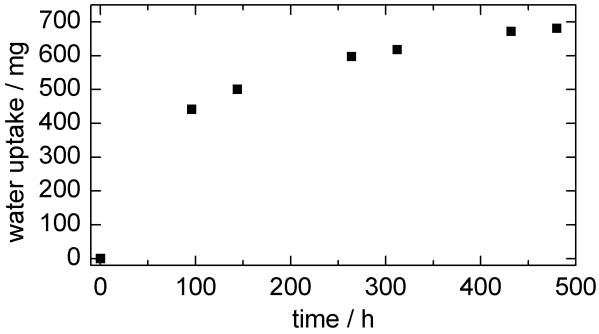

Figure 5: Water uptake versus time during the wetting of specimen D7 at 84 % RH.

Minor fluctuations of mass losses, noticed for nearly all samples, are explained by hygroscopic water uptake during weighing of samples previously dried at a very low humidity. However, the observed mass increase of the specimens A1, A6, C2, C4, C5 and D3–5 after the first cycle seems to be the result of pore clogging [11] and incomplete drying.

In general, a mass loss for successive cycling was not found, except for the specimens A8 and B4–B7. The slight mass loss in samples B4–B6 is in accordance with the observation that only slight sanding occurred on the surfaces of these specimens. Significant damage of the specimens of method A_{then} was only observed for the highest salt load (A8), it is important to note that the absence of damage for the next lower load (A7) might also be due to the low number of cycles. If and at which cycle damage occurs will be seen by further ongoing cycling. The mass loss of the specimens B_{mir} increases with increasing salt load. In contrast, a significant mass loss could not be detected for any of the specimens related to methods C_{mir} and D_{mir}, whatever the salt load, not even for sample D7 that broke down completely after the fourth cycle.

For the method D_{mir} it turns out that the expected condition of a solid state reaction was not fulfilled although the humidity was kept constantly below the deliquescence humidity of thenardite. The water uptake curve of specimen D7 is given as an example for all specimens of method D_{mir} in Figure 5. For sample D7 laden with 440 mg (3.09 mmol) of sodium sulfate, after drying a water uptake of 556 mg would be sufficient for the hydration of thenardite to mirabilite. The higher water uptake of about 695 mg provides evidence for the formation of a solution, explaining the aforementioned formation of efflorescences during cycling. However, this higher water uptake is not yet understood.

Both methods, C_{mir} and D_{mir}, involve a deliquescence–crystallization process. Considering the salt load, the observed damage confirms that method B_{mir}, the thenardite dissolution with liquid water and mirabilite crystallization, is the most harmful process. But regarding the pore filling ratio with respect to the crystalline phase the results could be interpreted differently. To discuss that more clearly the average mass losses,

calculated from the slope of the mass loss curves before the total breakdown, were plotted against the pore filling ratio for both crystalline phases in Figure 6. The average mass losses reflect sanding and crumbling of the specimens or in other words the superficial damage due to crystallization close to the surface.

Some scattering of the average mass loss is observed, which might be due to either the aforementioned error during weighing or due to pore clogging. However, significant values above 0.5 mg per g stone and cycle were only reached by the specimens A8, B4–B6. In case of the specimens A8, B6 and B7 the formation of cracks (Table 2) indicated that damage originated from the formation of subflorescences and their enlargement was accompanied by a mass loss. The specimens B4 and B5 were the only samples where the mass loss was produced solely by sanding of the surface, whilst the sticky behavior of the efflorescences noticed on the specimens related to methods C_{mir} and D_{mir} seems to prevent sanding.

Regarding the pore filling ratio it turns out that the damage caused by thenardite at 17.8 % pore filling (A8) is less than the damage observed for mirabilite crystallization at a pore filling of 51.6 % (B7) but more pronounced than at pore fillings of 23.1 % (B5) and 17.4 % (B4). In order to understand this result, a comparison of the effective stresses σ^*, calculated by Equation (2) [2], is useful.

$$\sigma^* = b \cdot \Phi \cdot \Delta p \qquad (2)$$

where b is the Biot coefficient, Φ the degree of pore filling with salt crystals, and Δp the theoretical crystallization pressure. The crystallization pressure for method A_{then} was calculated assuming that the growth of thenardite proceeds in contact with a solution saturated with respect to the better soluble Na_2SO_4 phase III [12]. This assumption seems quite reasonable because it is frequently observed that both solids, thenardite and phase III, can coexist during evaporation at low relative humidities [13,14,15]. It is important to note, that this is a minimum value for the supersaturation with respect to thenardite due to the unknown supersaturation of phase III necessary for its crystallization. In method B_{mir} the supersaturation with respect to mirabilite at a given temperature is given by the solubility of thenardite at the same temperature. A Biot coefficient of $b = 1$ was used in the calculations in lack of experimental values for Sand sandstone. It is important to note that average values of the pore filling ratio were used for the calculations yielding only a rough estimation of the effective stress. Due to salt transport during cycling, which was clearly more pronounced in method B_{mir} as in A_{then} (see Figures 3a and 3b), accumulation of salts can reveal higher pore filling ratios in some pores and in turn to higher effective stresses according to Equation (2). Average effective stresses σ^* are given in Table 3. Cracks were observed in those specimens (A8, B6, B7) where the average effective stress was higher than 4.27 MPa. Sanding occurred on the surfaces of

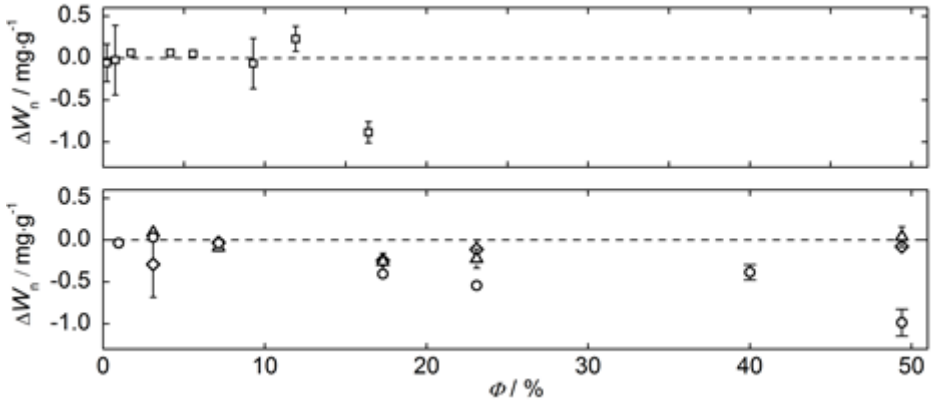

Figure 6: Average mass loss Δw_n per cycle versus pore filling ratio after impregnation with respect to thenardite in the upper diagram and mirabilite in the lower diagram. Squares represent method A_{then}, circles method B_{mir}, diamonds method C_{mir} and triangles method D_{mir}. Error bars reflects the standard deviation of the slope yielded by the linear regression. The dashed line is used as guide for the eye representing a mass loss of zero.

Table 3: Average effective stresses σ^* calculated for methods A_{then} and B_{mir} with the average pore filling ratios and the crystallization pressure (see text).

Specimen	σ^* (MPa) A_{then}	σ^* (MPa) B_{mir}
1	0.058	0.096
2	0.234	0.383
3	0.457	0.749
4	1.12	1.83
5	1.48	2.42
6	2.60	4.27
7	3.30	5.42
8	4.76	–(1)

(1) not tested

specimens B4 and B5 at average effective stresses of 1.83 MPa and 2.42 MPa. Due to the efflorescences observed on the surfaces of these specimens, the assumption of a salt enrichment closely beneath the surface is reasonable resulting in a higher effective stress near the surface than the calculated average value. The effective stresses may be

compared with the tensile strength of Sand sandstone. Values reported by different authors are quite scattered but most values reported are close to about 2 MPa [16,17,18]. This value is in reasonable agreement with our experimental observation and the calculated effective stresses.

In general it turns out that wetting with humid air is less harmful than wetting with liquid water, although the pore filling ratio with respect to mirabilite is the same as in the specimens of method B_{mir}. Hence, the average effective stress could be the same for the crystallization of mirabilite. As observed by Shahidzadeh and Desarnaud [13] in a capillary experiment, the precipitation of phase III and thenardite is more likely after dissolution via deliquescence than the crystallization of mirabilite. Hence, it is also possible that damage of the specimens treated with humid air (C_{mir} and D_{mir}) is caused by the crystallization of thenardite. In this case, the average effective stress would be the same as calculated for the specimens of method A_{then}. Up to now however, it is unclear which phases do actually crystallize within the porous network of Sand sandstone which will be the focus of future research. Therefore, an estimate of an average effective stress is more complicated. In addition, the appearance of a large amount of efflorescences yields a decrease of the average pore filling ratio resulting in a lower average effective stress. Contrarily, the salt accumulation due to salt transport during wetting leads to higher effective stresses in the pores with a higher salt load. Anyhow, the formation of cracks and the total breakdown observed for the specimen D7, give evidence that wetting with humid air at high salt loads can also be extremely destructive within few cycles.

4 Conclusion

In general the extreme destructiveness of the thenardite dissolution and mirabilite crystallization process (B_{mir}) is confirmed. The magnitude of damage increases with increasing salt load. Taking the degree of pore space filling with respect to the crystalline phase into account, it turns out that liquid wetting at 40 °C and subsequent drying, i.e. conditions where thenardite crystallization takes place, can cause more damage to Sand sandstone than mirabilite crystallization during wetting at 23 °C. The experiments carried out so far do not yet allow for an assessment of the influence of the pore filling ratio on the damage potential of thenardite. More insight is expected from our ongoing cycling experiments with the specimen A7. A study with even higher salt loads for cycling with liquid water (A_{then}) at 40 °C and for cycling including the deliquescence (C_{mir} and D_{mir}) has to be the subject of future research. Nonetheless, the study clearly reveals that the deliquescence of thenardite at high salt loads might also be very destructive at about 23 °C. Up to now it is unclear whether mirabilite or thenardite crystallization is responsible for the damage under such conditions.

Acknowledgement

This research was funded by Deutsche Forschungsgemeinschaft (DFG).

References

[1] Steiger M., Crystal Growth in porous materials. I: The crystallization pressure of large crystals. J. Cryst. Growth 282 (2005) 455-469.

[2] Espinosa-Marzal R. M. and Scherer G. W., Crystallization of sodium sulfate salts in limestone. Environ. Geol. 56 (2008) 605-621.

[3] Espinosa-Marzal R. M., Hamilton A., McNall M., Whitaker K. and Scherer G. W., The chemomechanics of crystallization during rewetting of limestone impregnated with sodium sulfate, J. Mater. Res. 26 (2011) 1472-1482.

[4] Linnow K., Niermann M., Bonatz D., Posern K. and Steiger M., Experimental studies of the mechanism and the kinetics of hydration reactions. Energ. Proc. 48 (2014) 394-404.

[5] Angeli M., Hébert R., Menéndez B., David C. and Bigas J.-P., Influence of temperature and salt concentration on the salt weathering of a sedimentary stone with sodium sulfate. Eng. Geol.115 (2010) 193-199.

[6] Tsui N., Flatt R. J. and Scherer G. W., Crystallization damage by sodium sulphate. J. Cult. Herit. 4 (2003) 109-115.

[7] Diaz Gonçalves T., Brito V., Alteration kinetics of natural stones due to sodium sulfate crystallization: can reality match experimental simulations? Environ. Earth Sci. (2014) doi: 10.1007/s12665-014-3085-0.

[8] Yu S., Oguchi C. T., Is sheer thenardite attack impotent compared with cyclic conversion of thenardite-mirabilite mechanism in laboratory simulation tests? Eng. Geol. 152 (2013) 148-154.

[9] Grimm W.-D., Bildatlas wichtiger Denkmalgesteine, Lipp-Verlag, München, 1990.

[10] Schäfer M., Steiger M., A rapid method for the determination of cation exchange capacities of sandstones: preliminary data. Geological Society Special Publication 52 (2002) 431–439.

[11] Espinosa-Marzal R. M., Scherer G. W., Impact of in-pore salt crystallization on transport properties. Eviron. Earth. Sci. 69 (2013) 2657-2669.

[12] Steiger M., Asmussen S., Crystallization of sodium sulfate phases in porous materials: The phase diagram Na_2SO_4–H_2O and the

generation of stress. Geochim. Cosmochim. Acta 72 (2008) 4291–4306.

[13] Shahidzadeh N., Desarnaud J., Damage in porous media: role of the kinetics of salt (re)crystallization. Eur. Phys. J. Appl. Phys. 60 (2012) 24205p1-p7.

[14] Linnow K., Steiger M., Lemster C., De Clerq H., Jovanovic M., In situ Raman observation of the crystallization in $NaNO_3$-Na_2SO_4-H_2O solution droplets. Environ. Earth Sci. 5 (2013) 1609-1620.

[15] Rodriguez-Navarro C., Doehne E., Sebastian E., How does sodium sulfate crystallize? Implications for the decay and testing of building materials, Cem. Concr. Res. 30 (2000) 1527-1534.

[16] Möller U., Thermo-hygrische Formänderungen und Eigenspannungen von natürlichen und künstlichen Mauersteinen. Dissertation University Stuttgart (2004).

[17] Alfes C., Bruchmechanisches Werkstoffverhalten von Sandstein unter Zugbeanspruchung. Dissertation RWTH Aachen, 1993.

[18] Siegesmund S., Dürrast H., Physical and mechanical properties of Rocks. In: Siegesmund S., Snethlage R. (eds.), Stone in Architecture. Springer, Berlin, 2011.